J Nanostruct 10(2): 202-212, Spring 2021

RESEARCH PAPER

Studies on Degradation of Dye Contamination using TiO_2/zeolite Modified with Nanocomposite. Influence of the Substitution on Photocatalytic Behaviour

Maryam Moosavifar * , Somayeh Ziaei

Department of Chemistry, Faculty of Science, University of Maragheh, Maragheh, Iran

ARTICLE INFO

Article History:
Received 29 December 2020
Accepted 18 January 2021
Published 01 April 2021

Keywords:
Chemical oxygen demand (COD)
Photocatalyst
Substituted metalloporphyrin
TiO_2
Y zeolite

ABSTRACT

This research aimed to explain the preparation of functionalized-CeTPP/TiO_2/Y zeolite in the degradation of dye contaminant. For this purpose, at first porphyrin ring is functionalized with OH groups with various ratios. Then the functionalized metal-porphyrin is encapsulated using the zeolite synthesis method. The entering of TiO_2 is achieved by the impregnation method. The obtained photocatalyst systems are characterized by X-ray diffraction (XRD), Fourier transformation-infrared spectroscopy (FT-IR), field emission scanning electron microscopy (FESEM), and energy-dispersive X-ray (EDS) technique. It is found the functionalizing of the porphyrin ring with OH not only improved the photocatalytic behaviour but the reaction also can be occurred in the absence of H_2O_2. The effect of several parameters including catalyst loading, dye concentration, TiO_2/CeTPP-Y on degradation yield is investigated. Mineralization of organic dye was studied by the Chemical Oxygen Demand (COD) experiment. It is found the kinetic of the photodegradation process is pseudo-first-order. However, the mechanism of the reaction has been proposed.

How to cite this article
Moosavifar M and Ziaei S. Studies on Degradation of Dye Contamination using TiO2/zeolite Modified with Nanocomposite. Influence of the Substitution on Photocatalytic Behaviour . J Nanostruct, 2021; 11(2):202-212. DOI: 10.22052/JNS.2021.02.001

INTRODUCTION

Nitrophenols have been of considerable interest because they are used as intermediates in the synthesis of some organophosphorus pesticides, explosives, leather coloring agents, dyes, and some pharmaceuticals products. However, nitrophenols are known as toxic, inhibitory, and biorefractory organic compounds. Releasing these compounds into the environment and streams as the effluent of industrial wastewater has toxic effects on the ecosystem and human health due to their persistence in the environment [1-6]. Therefore, the elimination of nitrophenol is gaining extensive attention in the quest for efficient and benign conversion processes in the area of environmental management. The conventional approaches to the removal of dyes from wastewater are adsorption, oxidation, microbiological, photocatalysis, and so on [7-10]. Among them, photocatalytic decomposition of organic compounds in wastewater has attracted a great deal of attention due to the viewpoint of green chemistry [11-17]. The TiO_2 is one of the most effective photocatalysts for its photostability, generally biologically and chemically inert but the critical drawback is the large bandgap which limited its application [18-22]. Therefore, for solving this problem, using photosensitizer agents including metalloporphyrins is a good manner to overcome this disadvantage [1, 23].

* *Corresponding Author Email: m.moosavifar90@gmail.com*

Also, metalloporphyrin derivatives especially the strong anchoring groups (e.g. hydroxyl, carboxyl, and sulfonic acid groups) can form a strong covalent band facilitating the charge-transfer interaction and maximize the charge-injection efficiency [1].

However, it is a well-known fact that heterogenization of metal complexes on solids supports show several advantages including the long lifetime of catalyst, facile recovery, and easy separation of the catalyst [24-29]. Several studies on the synthesis and photocatalytic activity of encapsulated metal complexes such as iron (II) bipyridine supported on Na-Y zeolite have been reported the degradation of malachite green [30]. Fe-exchanged Y zeolite as a catalyst was used for degradation of the reactive dyes by catalytic wet hydrogen peroxide oxidation [31, 32]. photodegradation of 2,4-dichlorophenol and organic pollutant using metallophethalocyanine and supported substituted metallophethalocyanine on MCM-41 under light irradiation was reported [19, 33-35].

In all of AOP's processes, oxidation reagent requires for completion of the degradation of 4-NP. AOPs based on H_2O_2 produce highly reactive species $^{\cdot}OH$ and they degrade a broad range of organic materials. However, in the high concentration of H_2O_2, it leads to the formation of $HO_2^{\cdot}$ radical which in turn, acts as a scavenger of $^{\cdot}OH$ radicals and consequently it reduces the efficiency of photodegradation [36]. To overcome these disadvantages and to inhibition of the usage of oxidant, we wish to report the synthesis and physicochemical characterization of $CeTPP(OH)_n/TiO_2/NaY$ (n=0-4) nanocomposite. The photosensitized oxidation of 4-nitrophenol using this heterogeneous system is reported on a lab-scale for the first time. Besides, substituted metalloporphyrin with several stoichiometric ratios is synthesized. Moreover, by using substituted metalloporphyrin with OH group in a peripheral position, the photodegradation of 4-NP was performed without H_2O_2. Furthermore, by increasing the number of substituted metalloporphyrin, the efficiency of photodegradation is enhanced.

MATERIALS AND METHODS

All materials were of the commercial reagent grade and were purchased from Sigma-Aldrich, Merck, and Fluka, Mojallaly industrial Co, Loba chemie, and Arman sina. Pyrrole and benzaldehyde were distilled before use.

Preparation of $Ce(OH)_nTPP/TiO_2/NaY$

$H_2(OH)_nTPP$ was prepared using freshly distilled pyrrole (4 mmol,) and benzaldehyde-para hydroxybenzaldehyde (with various ratios from 0-4 mmol) in propionic acid as solvent.

Cerium (IV) tetraphenylporphyrin was prepared according to our previous works [37],[38]. $Ce(OH)_nTPP$ (n=0-4) (n indicates the number of OH hydroxyl groups on the peripheral ring) was synthesized inside the nanocage of NaY zeolite by hydrothermal treatment [39]. The aluminosilicate gel was prepared by stirring colloidal silica (2.3 g), sodium hydroxide (3.1 g), sodium aluminate (1.6 g), and H_2O (40 mL). After then, $Ce(OH)_nTPP$ (0.02 g, 3.6×10^{-4} mol) was added. The crystallization occurred at 95°C under static conditions in a stainless steel bomb (250 mL) for 48 h. The adsorbed complexes on the external surface of the zeolite were removed through Soxhlet extractions with di-Chloromethane, ethanol, and acetone. The final product was dried at 80°C for 24 h.

To encaging TiO_2 on zeolite structure, 1 g $CeTPP(OH)_n/NaY$ was added to the suspension containing 0.16 g TiO_2 in 50 mL distilled water with stirring for 36 h. Then, the solvent was evaporated under vacuum and dried at 100 °C for 12 h. The obtained materials were calcinated at 523 K for 5 h.

General procedure for the photodegradation of 4-Nitrophenol

For this purpose, a 0.02 g catalyst was added to the solution of 50 mL of 4-Nitrophenol (4×10^{-5} M) and then stirred at the dark to obtain adsorption/desorption equilibrium to eliminate the error due to any initial adsorption effect. After that, the irradiation experiments were carried out in the presence of H_2O_2 in a photocatalyst reactor. In another typical procedure, the photodegradation reaction was performed in the absence of H_2O_2 to investigate the OH effect in the peripheral position of the porphyrin ring on the photodegradation process. The suspension was magnetically stirred during irradiation. Also, to monitor the 4-Nitrophenol degradation process, about 3 mL of the suspension was withdrawn and the photocatalysts were separated from the suspension by filtration. Finally, the reaction progress was monitored by its characteristic

absorption band at 317 nm using a double-beam UV-Visible spectrometer.

Chemical oxygen demand

Chemical oxygen demand (COD) is a measure of the amount of the required oxygen for decomposing organic matter. This indicates an aggregate measure of the organic compounds that can be oxidized to inorganic (mineral) materials at the end of the reaction. Therefore, it was used to evaluate the degree of mineralisation that had occurred during the photocatalytic process. The COD at the beginning and the end of the experimental runs was determined by volumetric titration methodology [40].

RESULTS AND DISCUSSION

Preparation and characterization of CeTPP(OH)$_n$/TiO$_2$/NaY

The synthesis of zeolite-encapsulated (OH)$_n$-substituted cerium (IV) tetraphenylporphyrin (ZECTPP(OH)$_n$) is carried out by the zeolite synthesis method. In this method, the anionic template was synthesized around the cationic guest using an electrostatic interaction. Clearly, this method is a clean synthesis way since there isn't any free metal ion, free ligand, and other impurities in the zeolite cages, and therefore, the characterization of catalyst seems easy. The crude material was treated with Soxhlet extraction with ethanol, dichloromethane, and acetone to remove the excess ligand and external surface adsorbed complexes. Encaging of TiO_2 in zeolite cage performed by impregnation method. The Ce and Ti content of the photocatalyst is determined by ICP methods (Table 1). The results show that TiO_2 amounts in all of the samples are similar that proves the TiO_2/catalyst ratio is constant.

The XRD patterns of the photocatalysts in Fig. 1 indicate that all synthesized catalysts have crystallinity almost identical to that of the parent NaY zeolite with ICDD file no. 083-1084. The presence of the characteristic peaks at 2θ=25, 37, and 46° related to the anatase phase of TiO_2, also proves the insertion of TiO_2 into the pores of the zeolite. However, the peak in the region of 2θ=12° can be related to metalloporphyrin species. In addition, the intensity of the main peak in the zeolite structure remained unchanged, which indicating the preservation of the framework and crystallinity of zeolite upon encapsulation of cerium (IV) porphyrin into its supercages.

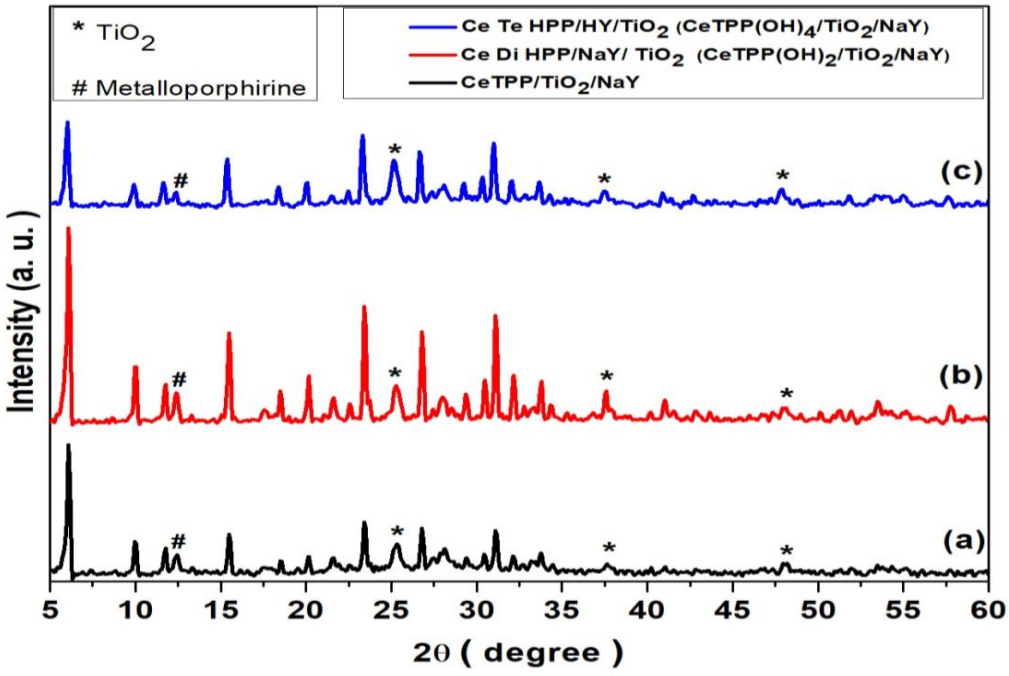

Fig. 1. XRD patterns of a) CeTPP/TiO_2/NaY, b) Ce Di HPP/NaY/ TiO_2 (CeTPP(OH)$_2$/TiO_2/NaY), c) Ce Te HPP/HY/TiO_2 (CeTPP(OH)$_4$/TiO_2/NaY)

Table 1. The percentage of Ce and Ti in the photocatalysts species

Entry		Ce (%)	Ti (%)
1	CeTPP/TiO_2/NaY	4.4	7.8
2	Ce Mo HPP/NaY/ TiO_2	3.73	8.6
3	Ce Di HPP/NaY/ TiO_2	4.7	8.5
4	Ce Tr HPP/NaY/ TiO_2	3.8	7.6
5	Ce Te HPP/NaY/ TiO_2	0.2	8

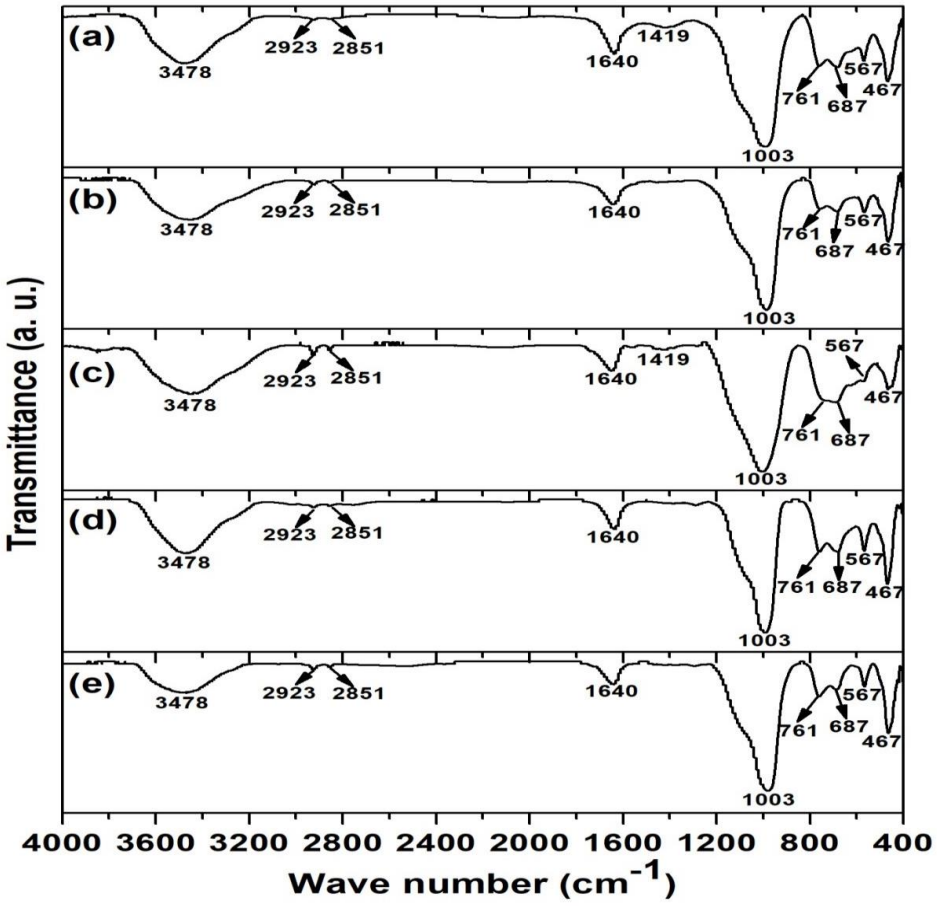

Fig. 2. FT-IR spectra of a) Ce(TPP)/NaY/TiO_2, b) CeMoHPP/NaY/TiO_2 (CeTPP(OH) / TiO_2/NaY), c) CeDiHPP/NaY/ TiO_2 ($CeTPP(OH)_2$/TiO_2/NaY), d) CeTrHPP/HY/TiO_2 ($CeTPP(OH)_3$/TiO_2/NaY), e) CeTeHPP/HY/TiO_2 ($CeTPP(OH)_4$/ TiO_2/NaY)

It confirmed that the catalyst distributed as fine particles in the zeolite pores. Moreover, by functionalizing the porphyrin rings, the XRD pattern preserved except for the slight change that proved the presence of OH group in peripheral position is without any steric spatial. However, reflections in the regions of (2 2 0), (3 1 1), and (3 3 1) are related to the location of cations. Upon the encapsulation of complexes in the cages of zeolite, the order of relative peak intensities changes from

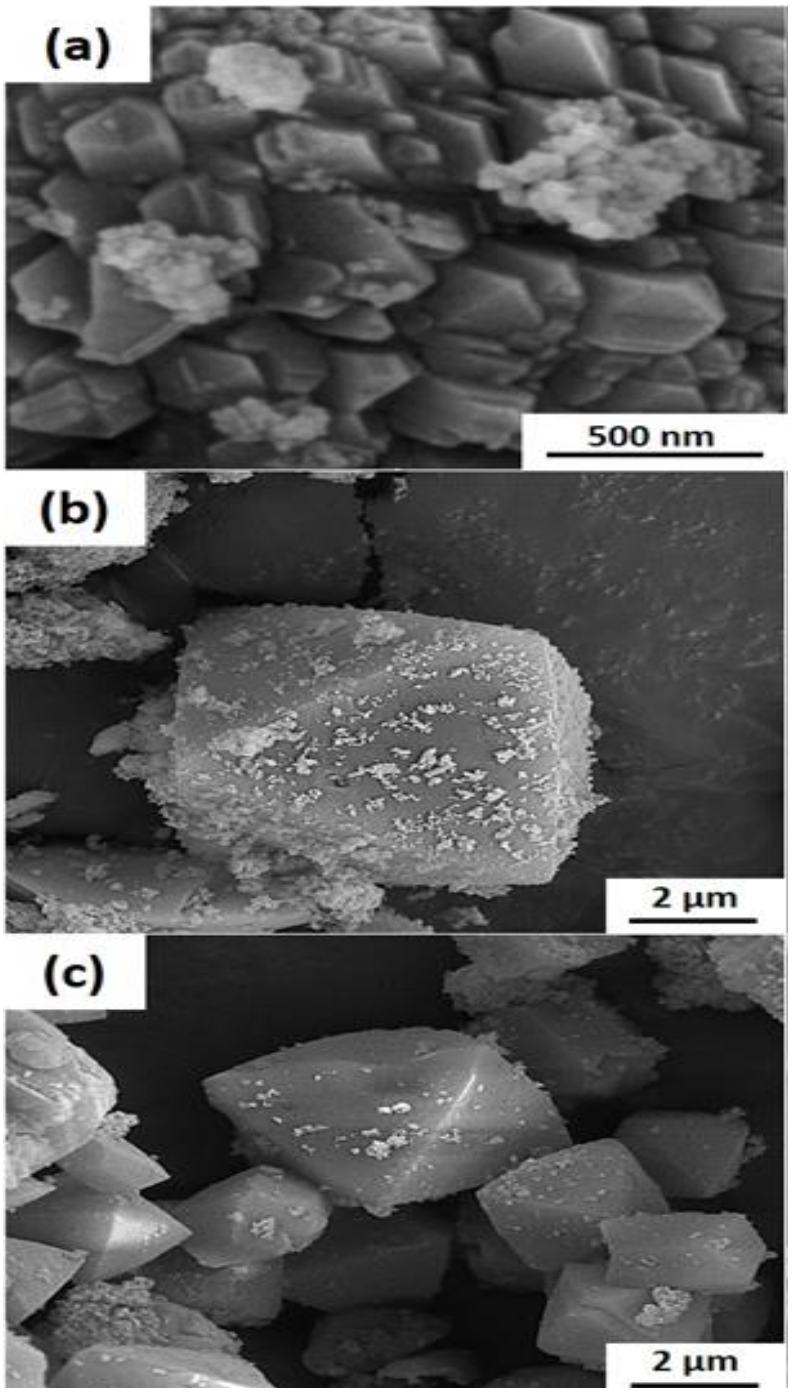

Fig. 3. FESEM micrograph of a) CeTPP/TiO_2/NaY, b) Ce Di HPP/NaY/TiO_2 ($CeTPP(OH)_2$/TiO_2/NaY), and c) CeTeHPP/NaY/TiO_2($CeTPP(OH)_4$/TiO_2/NaY)

(3 3 1) > (2 2 0) > (3 1 1) to (3 3 1) > (3 1 1) > (2 2 0) which is confirmed the substitution of Na^+ ions by Ce^{4+} ions. Then, a rearrangement occurs during the complexation [41].

The FT-IR spectra of NaY, CeTPP/TiO_2/NaY and CeTPP(OH)$_n$/TiO_2/NaY zeolite are shown in Fig. 2. No shift observes in the position of the zeolite lattice bands in the encapsulated metalloporphyrins. However, bands in accordance with cerium porphyrin observe. In these spectrums, the bands in the range 450–1200 cm^{-1} are attributed to the strong zeolite lattice vibration, and bands in 3200–3600 cm^{-1} and 1636 cm^{-1} are due to lattice water molecules and the surface hydroxyl groups. Band in region 2900 cm^{-1} and 1150-1500 cm^{-1} is in accordance to C-H and C-C, and C-N vibration respectively indicates the presence of metallocomplexes into zeolite cage [38],[42]. Also, a peak in the region 2922 cm^{-1} is related to O-H vibration in the peripheral porphyrin situation which its intensity is increased with enhancing of substituted ring number (Fig. 2b, c, d, e). Besides, peaks in the 800-890 cm^{-1} are related to the M–O–M vibrations (where M=Si, Al, Ce, and Ti) [43]. Meanwhile, absorption bands in the region of 860-920 cm^{-1} can be related to the TiO_2 species stretching vibration that masked by zeolite structures [16].

Fig. 3 shows the field emission scanning electron micrograph (FESEM) of the CeTPP(OH)$_n$/TiO_2/NaY zeolite with the cubo-octahedral units. Based on encapsulation of metallocomplex, the morphology of zeolite remained unchanged confirmed in the template synthesis method, metallocomplexes act as a template, and the zeolite structure formed around it. Moreover, the presence of some species in nanometer size proved the insertion of TiO_2 into the pores of zeolite (Fig. S1).

Further, the FESEM-EDX spectrum of CeTPP(OH)$_n$/TiO_2/NaY nanocomposite showed the presence of a component of the photocatalyst. Thus, it demonstrated the formation of metallocomplexes into zeolite cages (Fig. S2).

The transmission electron micrograph (TEM) of CeTeHPP / NaY / TiO_2 is shown in Fig. 4, showing uniform Cubo-octahedral units that encompassed the supercages.

Investigation of photocatalytic activity of CeTPP/TiO_2/NaY

To detect the photocatalytic activity of CeTPP/TiO_2/NaY, degradation of 4-Nitrophenol is tested as a function of different experimental parameters are presented in Figs. 5(a-d).

The effect of catalyst amount on the removal of 4-Nitrophenol was studied by varying the catalyst

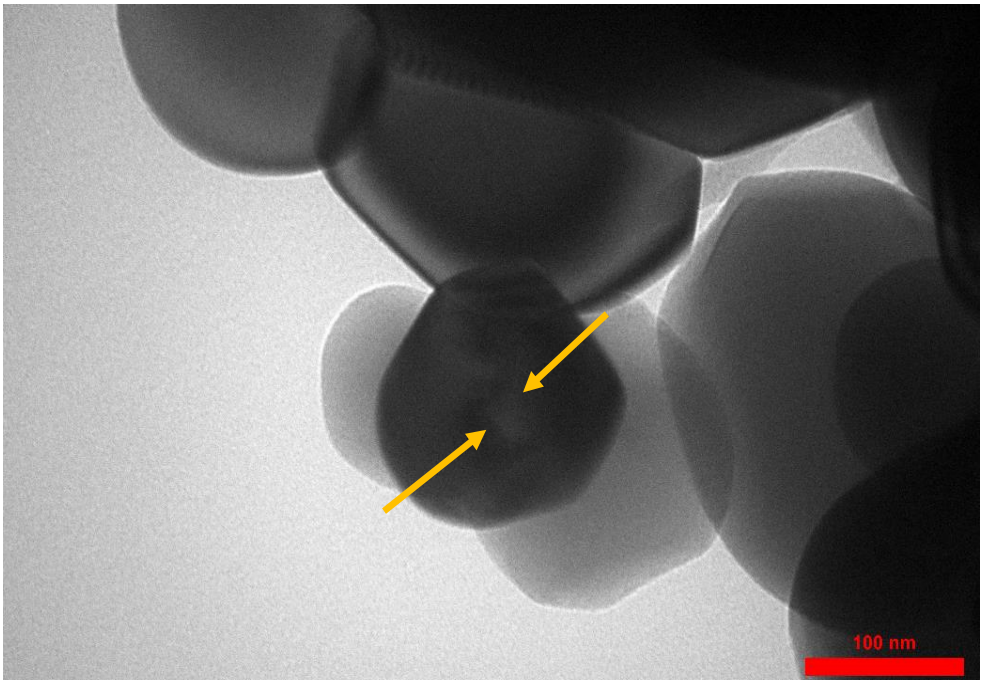

Fig. 4. TEM micrograph of CeTeHPP/NaY/TiO_2

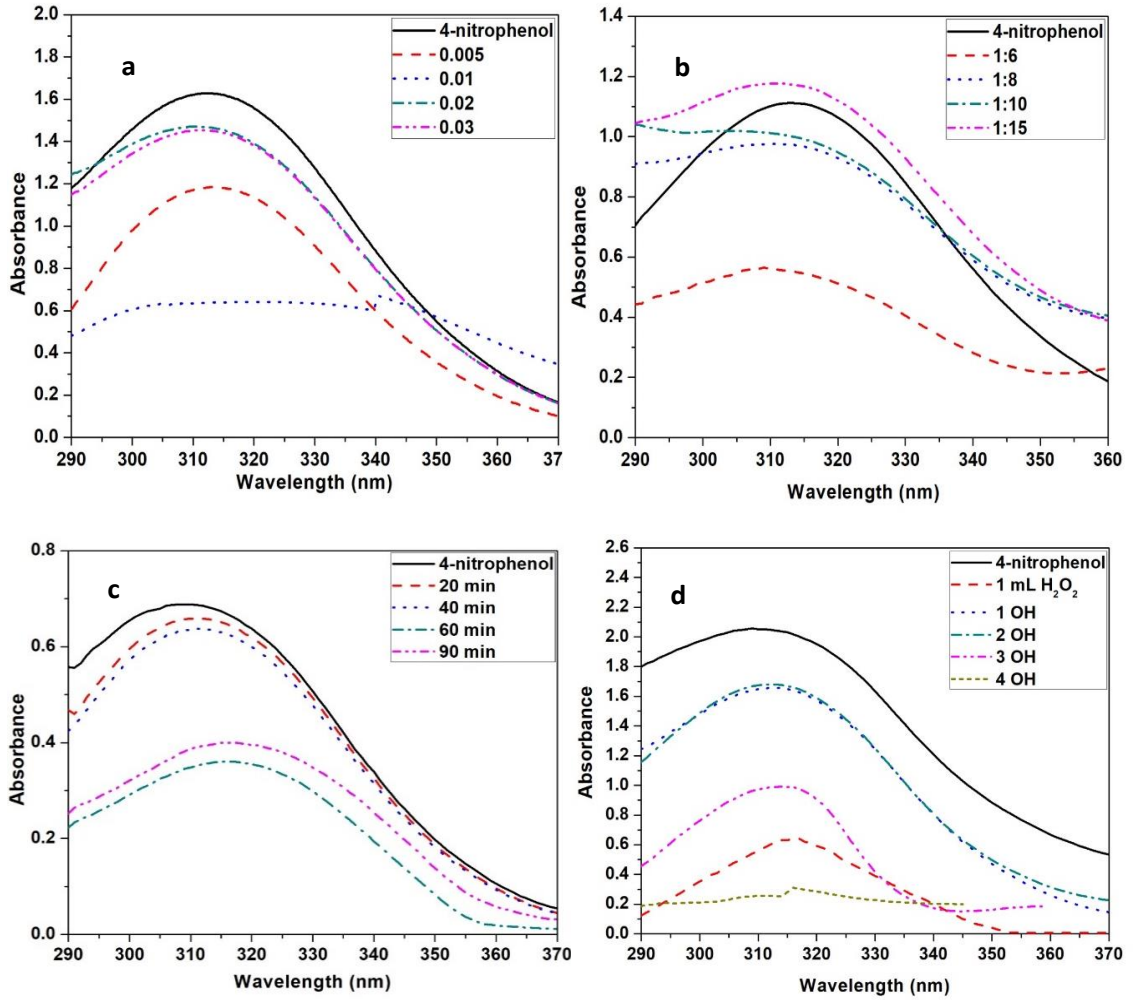

Fig. 5. (a) Effect of catalyst amount on the photodegradation of 4-NP, (b) Effect of TiO_2/catalyst ratio on the photodegradation of 4-NP, (c) Effect of time reaction on the photodegradation of 4-NP, (d) Effect of substituted group number on the photodegradation of 4-NP

amount from 0.005 to 0.03 g. The results collected in Fig.5a. We found that with an increase amount of the catalyst, degradation of 4-Nitrophenol was enhanced because of an increase in the absorption of dye molecules. However, the optimum degradation was obtained with a 0.01 g catalyst. At high catalyst loading, aggregation of species increases, in turn, reduces the catalytic activity of the photocatalyst because of the turbidity of the solution [17], [44].

To obtain the optimum ratio, a variety of TiO_2/ catalyst ratio including 1:6, 1:8, 1:10, 1:15 tested in the photodegradation of dye molecules. The results showed that the maximum photocatalytic activity was obtained with 1:6 ratios. It seems with increasing TiO_2 amount, the reduction between catalyst and dye occurred which followed by decreasing in the interfacial area between the reaction solution and the photocatalyst. Consequently, the degradation of 4-NP reduced [43] (Fig. 5b). To study the catalytic activity of CeTPP/TiO_2/NaY and the role of H_2O_2 in catalytic oxidation of dye, dye degradation experiments with different values of H_2O_2 were carried out. It suggests that a system with 1 mL H_2O_2 gives maximum removal of 4-NP. So, upon increasing in H_2O_2 value, the removal of dye decreases. It is likely due to the higher concentration of H_2O_2 since it acts as a scavenger and then, photocatalytic activity is disrupted. It seems that in the higher concentration of H_2O_2, the main part of $^{\cdot}OH$ radicals have been consumed by H_2O_2 which was followed by the formation of less reactive $HO_2^{\cdot}$ radical [45]. Finally, photodegradation of 4-NP

Table 2. Comparison of the efficiency of various catalysts in the photodegradation of para-Nitrophenol

Entry	Catalyst	Removal (%)	Reaction conditions	Ref
1	FeTPP/NaY	85	4-Np 50mL, 2×10^{-4} M , catalyst 40 mg, pH= 6.5, H_2O_2 2 mM, 2 h reaction time	[36]
2	Cesalophen/TiO_2/zeolite	80	4-Np 25mL, 1×10^{-4} M , catalyst 10 mg, pH= 7, H_2O_2 1 mL, UV condition, 2 h reaction time	[46]
3	$NiCo_2O_4$-$Bi_2O_2CO_3$ composite	97	4-NP 100 ppm, catalyst 0.4 g, pH=6, Microwave condition, 7 min	[47]
4	metalloporphyrins-modified TiO_2 composites (MDHPP–TiO_2)(M=Cu, Zn, Co)	65-90	4-NP 20 mg/L, catalyst 0.3 g/L, pH=7.3, 5h reaction time	[48]
5	Montmorillonite clay Fe, Al-PILC(8.1%WT Fe)	70	4-NP 1 mmol, catalyst 1g/L, 10mM H_2O_2, 5 h reaction time	[49]
6	Fenton process	99	1 mM 4-NP, catalyst 5 mg/L Fe^{2+}, pH 3,10 mM H_2O_2 , 2 h reaction time	[50]
7	Mn(II)- MCM-41	70	1 mM 2-NP, Catalyst 2 g L^{-1}, 1 mM H_2O_2, 80 ◦C, pH 3, 5 h reaction time	[51]
8	Nano-SCH	91	nano–SCH–0.125, 60 min, H_2O_2, 298K	[52]
9	Collagen-(AMPS-MAA/AAm)-Fe_3O_4@SiO_2	83	PH=7, 4-NP, qm=19.2 mg/g	[53]
10	$Ce(OH)_n$TPP/TiO_2/NaY		4-Np 50mL, 5×10^{-5} M , catalyst:TiO_2 1:6, 10 mg, H_2O_2 1 mL, 1 h reaction time	This work

reduces (Fig. S3). Under the optimum conditions, photodegradation of 4-NP is investigated in the presence of CeTPP$(OH)_n$/TiO_2/NaY catalyst under optimum conditions. The obtained results are displayed in Fig. 5c. The reaction is completed within one hour, and after that, more removal of dye did not occur.

To investigate and compare the effect of OH group anchored to porphyrin ring on photodegradation process, the reaction is performed in the absence of H_2O_2 with the various ratios of substituted metalloporphyrin and the presence of 1 mL H_2O_2 with net metalloporphyrin. The results revealed that by increasing OH-substituted porphyrin number, photodegradation yield enhanced so that the photodegradation yield in the presence of CeTPP$(OH)_4$/TiO_2/NaY without H_2O_2 become better than CeTPP/TiO_2/NaY with 1 mL H_2O_2. It seems that OH in the peripheral position of the porphyrin ring can be broken as hemolytic and act as ·OH radical obtained from H_2O_2 which it is the driving force for AOP's processes (Fig. 5d).

Moreover, Table. 2 shows the efficiency of our catalytic system with the efficiency of some other catalysts in the photodegradation of 4-NP. It is clear that our catalyst is a mild, effective with high efficiency system.

Mineralization of 4-NP upon the photodegradation reactions is established by COD analysis. It is observed that the obtained solution after completing the photodegradation reaction shows a significant COD removal (53.2%) for CeTPP/TiO_2/NaY and 57% for CeTPP$(OH)_4$/TiO_2/NaY after 60 min irradiation. Thus it proved that a part of the organic material is mineralized. This, in turn, indicates that the mineralization of 4-NP is followed by the formation of simple inorganic materials such as carbon dioxide and water during photodegradation.

CONCLUSION

In this study, the preparation of $CeTPP(OH)_n$/TiO_2/NaY catalyst was performed using zeolite synthesis and impregnation methods respectively. XRD studies show that upon the incorporation of the metal complex, crystallinity of the zeolite matrix remains unchanged. In addition, the appearance of the peak in the 2θ=25 indication of TiO_2 proved the insertion of TiO_2 in nanopores of zeolite. Also, the catalyst displays an efficient photoactivity for the degradation 4-Nitrophenol in the presence of H_2O_2 under UV illumination. Interestingly, the best results are obtained within 1 h for a concentration of 5×10^{-5} of 4-NP, 1:6 catalyst/TiO_2, the amount of catalyst loading about 0.01 g and, 1 mL H_2O_2 under UV irradiation. In addition, the photodegradation process is performed by OH-substituted porphyrin encapsulated into zeolite NaY, and TiO_2 in the absence of H_2O_2 and the results were in the better yield.

ACKNOWLEDGEMENT

We are grateful from Maragheh University for support this work.

CONFLICT OF INTEREST

The authors declare that there are no conflicts of interest regarding the publication of this manuscript.

REFERENCES

1. Sun W, Li J, Lü X, Zhang F. Preparation, characterization and photocatalytic activity of metalloporphyrins-modified TiO2 composites. Research on Chemical Intermediates. 2012;39(3):1447-57.
2. Kidak R, Ince NH. Ultrasonic destruction of phenol and substituted phenols: A review of current research. Ultrasonics Sonochemistry. 2006;13(3):195-9.
3. Hoffmann MR, Martin ST, Choi W, Bahnemann DW. Environmental Applications of Semiconductor Photocatalysis. Chemical Reviews. 1995;95(1):69-96.
4. Dieckmann MS, Gray KA. A comparison of the degradation of 4-nitrophenol via direct and sensitized photocatalysis in TiO2 slurries. Water Research. 1996;30(5):1169-83.
5. Noroozi Z, Ali Rasekh H, Jaafar Soltanianfard M. Preparation and characterization of ZrO2-Cr2O3 nanocomposite as a p-n heterojunction by a facile sol-gel method: A kinetic investigation on the removal of p-nitrophenol dye from aqueous media. Polyhedron. 2019;168:11-20.
6. Yang Q, Guo E, Liu H, Lu Q. Engineering of Z-scheme 2D/3D architectures with Bi2MoO6 on TiO2 nanosphere for enhanced photocatalytic 4-nitrophenol degradation. Journal of the Taiwan Institute of Chemical Engineers. 2019;105:65-74.
7. Low KS, Lee CK, Wong AM. Carbonized spent bleaching earth as a sorbent for some organic dyes. Journal of Environmental Science and Health Part A: Environmental Science and Engineering and Toxicology. 1996;31(3):673-85.
8. Huang CP, Dong C, Tang Z. Advanced chemical oxidation: Its present role and potential future in hazardous waste treatment. Waste Management. 1993;13(5-7):361-77.
9. Ogunbayo TB, Antunes E, Nyokong T. Investigation of homogeneous photosensitized oxidation activities of palladium and platinum octasubstituted phthalocyanines: Oxidation of 4-nitrophenol. Journal of Molecular Catalysis A: Chemical. 2011;334(1-2):123-9.
10. Li X, Wang J, Li M, Jin Y, Gu Z, Liu C, et al. Fe-doped TiO 2 /SiO 2 nanofibrous membranes with surface molecular imprinted modification for selective photodegradation of 4-nitrophenol. Chinese Chemical Letters. 2018;29(3):527-30.
11. Fox MA, Doan KE, Dulay MT. The effect of the "Inert" support on relative photocatalytic activity in the oxidative decomposition of alcohols on irradiated titanium dioxide composites. Research on Chemical Intermediates. 1994;20(7):711-21.
12. Bahnemann D, Cunningham J, Fox M, Pelizzetti E, Pichat P, Serpone N, et al. Aquatic and surface photochemistry. Lewis, Boca Raton, FL. 1994:261.
13. Abdullah M, Low GKC, Matthews RW. Effects of common inorganic anions on rates of photocatalytic oxidation of organic carbon over illuminated titanium dioxide. The Journal of Physical Chemistry. 1990;94(17):6820-5.
14. Sabate J, Anderson MA, Aguado MA, Giménez J, Cervera-March S, Hill CG. Comparison of TiO2 powder suspensions and TiO2 ceramic membranes supported on glass as photocatalytic systems in the reduction of chromium(VI). Journal of Molecular Catalysis. 1992;71(1):57-68.
15. Sabate J, Anderson M, Kikkawa H, Edwards M, Hill C. A kinetic study of the photocatalytic degradation of 3-chlorosalicylic acid over TiO 2 membranes supported on glass. Journal of catalysis. 1991;127(1):167-177.
16. Kim Y, Yoon M. TiO2/Y-Zeolite encapsulating intramolecular charge transfer molecules: a new photocatalyst for photoreduction of methyl orange in aqueous medium. Journal of Molecular Catalysis A: Chemical. 2001;168(1-2):257-63.
17. Aravindhan R, Fathima NN, Rao JR, Nair BU. Wet oxidation of acid brown dye by hydrogen peroxide using heterogeneous catalyst Mn-salen-Y zeolite: A potential catalyst. Journal of Hazardous Materials. 2006;138(1):152-9.
18. Lopez L, Daoud WA, Dutta D. Preparation of large scale photocatalytic TiO2 films by the sol–gel process. Surface and Coatings Technology. 2010;205(2):251-7.
19. Zanjanchi MA, Ebrahimian A, Arvand M. Sulphonated cobalt phthalocyanine–MCM-41: An active photocatalyst for degradation of 2,4-dichlorophenol. Journal of Hazardous Materials. 2010;175(1-3):992-1000.
20. Linsebigler AL, Lu G, Yates JT. Photocatalysis on TiO2 Surfaces: Principles, Mechanisms, and Selected Results. Chemical Reviews. 1995;95(3):735-58.
21. Klosek S, Raftery D. Visible Light Driven V-Doped TiO2 Photocatalyst and Its Photooxidation of Ethanol. The Journal of Physical Chemistry B. 2001;105(14):2815-9.
22. Al-Qaradawi S, Salman SR. Photocatalytic degradation of methyl orange as a model compound. Journal of Photochemistry and Photobiology A: Chemistry. 2002;148(1-3):161-8.

23. Rajamanickam D, Shanthi M. Photocatalytic degradation of an organic pollutant by zinc oxide – solar process. Arabian Journal of Chemistry. 2016;9:S1858-S68.
24. Liu X, Iu K-K, Kerry Thomas J. Encapsulation of TiO2 in zeolite Y. Chemical Physics Letters. 1992;195(2-3):163-8.
25. Liu X, Iu K-K, Thomas JK. Preparation, characterization and photoreactivity of titanium(IV) oxide encapsulated in zeolites. Journal of the Chemical Society, Faraday Transactions. 1993;89(11):1861.
26. Anpo M, Yamashita H, Ichihashi Y, Fujii Y, Honda M. Photocatalytic Reduction of CO2 with H2O on Titanium Oxides Anchored within Micropores of Zeolites: Effects of the Structure of the Active Sites and the Addition of Pt. The Journal of Physical Chemistry B. 1997;101(14):2632-6.
27. Saladin F, Kamber I, Pfanner K, Calzaferri G. Photochemical water oxidation to oxygen at the solid/gas interface of AgCl on zeolite A. Journal of Photochemistry and Photobiology A: Chemistry. 1997;109(1):47-52.
28. Yamashita H, Ichihashi Y, Anpo M, Hashimoto M, Louis C, Che M. Photocatalytic Decomposition of NO at 275 K on Titanium Oxides Included within Y-Zeolite Cavities: The Structure and Role of the Active Sites. The Journal of Physical Chemistry. 1996;100(40):16041-4.
29. Moosavifar M, Bagheri S. Photocatalytic Performance of H 6 P 2 W 18 O 62 /TiO 2 Nanocomposite Encapsulated into Beta Zeolite under UV Irradiation in the Degradation of Methyl Orange. Photochemistry and Photobiology. 2018;95(2):532-42.
30. Neamţu M, Zaharia C, Catrinescu C, Yediler A, Macoveanu M, Kettrup A. Fe-exchanged Y zeolite as catalyst for wet peroxide oxidation of reactive azo dye Procion Marine H-EXL. Applied Catalysis B: Environmental. 2004;48(4):287-94.
31. Alvaro M, Carbonell E, Esplá M, Garcia H. Iron phthalocyanine supported on silica or encapsulated inside zeolite Y as solid photocatalysts for the degradation of phenols and sulfur heterocycles. Applied Catalysis B: Environmental. 2005;57(1):37-42.
32. Neamţu M, Catrinescu C, Kettrup A. Effect of dealumination of iron(III)—exchanged Y zeolites on oxidation of Reactive Yellow 84 azo dye in the presence of hydrogen peroxide. Applied Catalysis B: Environmental. 2004;51(3):149-57.
33. Mohamed RM, Mohamed MM. Copper (II) phthalocyanines immobilized on alumina and encapsulated inside zeolite-X and their applications in photocatalytic degradation of cyanide: A comparative study. Applied Catalysis A: General. 2008;340(1):16-24.
34. Wang Z, Mao W, Chen H, Zhang F, Fan X, Qian G. Copper(II) phthalocyanine tetrasulfonate sensitized nanocrystalline titania photocatalyst: Synthesis in situ and photocatalysis under visible light. Catalysis Communications. 2006;7(8):518-22.
35. DeOliveira E, Neri CR, Ribeiro AO, Garcia VS, Costa LL, Moura AO, et al. Hexagonal mesoporous silica modified with copper phthalocyanine as a photocatalyst for pesticide 2,4-dichlorophenoxiacetic acid degradation. Journal of Colloid and Interface Science. 2008;323(1):98-104.
36. Moosavifar M, Heidari SM, Fathyunes L, Ranjbar M, Wang Y, Arandiyan H. Photocatalytic Degradation of Dye Pollutant Over FeTPP/NaY Zeolite Nanocomposite. Journal of Inorganic and Organometallic Polymers and Materials. 2019;30(5):1621-8.
37. Moosavifar M, Alemi A, Marefat MR, Nouruzi N, Mahmoodi H. The effect of synthesis method and post-synthesis treatment on the formation of neutral Mn(II) complex into anionic zeolite structure and investigation of its catalytic activity in the epoxidation of alkenes. Journal of the Iranian Chemical Society. 2014;11(6):1561-7.
38. Moghadam M, Tangestaninejad S, Mirkhani V, Mohammadpoor-Baltork I, Moosavifar M. Host (nanocavity of zeolite-Y or X)–guest (manganese (III) tetrakis[4-N-methylpyridinum]porphyrin) nanocomposite materials as efficient catalysts for biomimetic alkene epoxidation with sodium periodate: Shape-selective epoxidation of linear alkenes. Journal of Molecular Catalysis A: Chemical. 2009;302(1-2):68-75.
39. Rosa ILV, Manso CMCP, Serra OA, Iamamoto Y. Biomimetical catalytic activity of iron(III) porphyrins encapsulated in the zeolite X. Journal of Molecular Catalysis A: Chemical. 2000;160(2):199-208.
40. APHA A. WEF (American Public Health Association, American Water Works Association, and Water Environment Federation). 1998. Standard methods for the examination of water and wastewater.19.
41. Linde C, Anderlund MF, Åkermark B. The effect of phenolates in the (salen)Mn-catalyzed epoxidation reactions. Tetrahedron Letters. 2005;46(33):5597-600.
42. Nakagaki S, Xavier CR, Wosniak AJ, Mangrich AS, Wypych F, Cantão MP, et al. Synthesis and characterization of zeolite-encapsulated metalloporphyrins. Colloids and Surfaces A: Physicochemical and Engineering Aspects. 2000;168(3):261-76.
43. Anandan S, Ryu SY, Cho W, Yoon M. Heteropolytungstic acid (H3PW12O40)—encapsulated into the titanium-exchanged HY (TiHY) zeolite: a novel photocatalyst for photoreduction of methyl orange. Journal of Molecular Catalysis A: Chemical. 2003;195(1-2):201-8.
44. San N, Hatipoğlu A, Koçtürk G, Çınar Z. Photocatalytic degradation of 4-nitrophenol in aqueous TiO2 suspensions: Theoretical prediction of the intermediates. Journal of Photochemistry and Photobiology A: Chemistry. 2002;146(3):189-97.
45. Legrini O, Oliveros E, Braun AM. Photochemical processes for water treatment. Chemical Reviews. 1993;93(2):671-98.
46. Moosavifar M, Nikkhoo M, Mansouri F. Host (nanocavity of dealuminated Y zeolite)-guest (Ce(IV) salophen/TiO2) nanocomposite materials as an efficient photocatalyst for degradation of 4-nitrophenol. Research on Chemical Intermediates. 2016;42(10):7417-27.
47. Xu W, Chen J, Qiu Y, Peng W, Shi N, Zhou J. Highly efficient microwave catalytic oxidation degradation of 4-nitrophenol over magnetically separable NiCo2O4-Bi2O2CO3 composite without adding oxidant. Separation and Purification Technology. 2019;213:426-36.
48. Ji K, Arandiyan H, Liu P, Zhang L, Han J, Xue Y, et al. Interfacial insights into 3D plasmonic multijunction nanoarchitecture toward efficient photocatalytic performance. Nano Energy. 2016;27:515-25.
49. Sun W, Li J, Lü X, Zhang F. Preparation, characterization and photocatalytic activity of metalloporphyrins-modified TiO2 composites. Research on Chemical Intermediates. 2012;39(3):1447-57.
50. Arandiyan H, Chang H, Liu C, Peng Y, Li J. Dextrose-aided hydrothermal preparation with large surface area on 1D single-crystalline perovskite La0.5Sr0.5CoO3 nanowires without template: Highly catalytic activity for methane

combustion. Journal of Molecular Catalysis A: Chemical. 2013;378:299-306.
51. Uberoi V, Bhattacharya SK. Toxicity and degradability of nitrophenols in anaerobic systems. Water Environment Research. 1997;69(2):146-56.
52. Qiao XX, Yu K, Xu JY, Cai YL, Li YF, Cao HL, et al. Engineered nanoscale schwertmannites as Fenton–like catalysts for highly efficient degradation of nitrophenols. Applied Surface Science. 2021;548:149248.
53. Nakhjiri MT, Bagheri Marandi G, Kurdtabar M. Preparation of magnetic double network nanocomposite hydrogel for adsorption of phenol and p-nitrophenol from aqueous solution. Journal of Environmental Chemical Engineering. 2021;9(2):105039.